7.3 Slow Modulation

So far we have considered neuronal models having voltage- or Ca^{2+}-gated conductances operating on a fast time scale comparable with the duration of a spike. Such conductances participate directly or indirectly in the generation of each spike and subsequent repolarization of the membrane potential. In addition, neurons have dendritic trees and some slow conductances and currents that are not involved in the spike-generation mechanism, but rather modulate it. For example, some cortical pyramidal neurons have $I_{\rm h}$, all thalamocortical neurons have $I_{\rm h}$ and $I_{\rm Ca(T)}$. Activation and inactivation kinetics of these current is too slow to participate in the generation of up-stroke or downstroke of a spike, but the currents can modulate spiking, e.g., they can transform it into bursting.

To illustrate the phenomenon of slow modulation, we use the $I_{\rm Na,p}$+$I_{\rm K}$ +$I_{\rm K(M)}$-model

$$\begin{array}{ll} C\dot{V} & = \overbrace{I - g_{\rm L}(V-E_{\rm L}) - g_{\rm Na} m_\infty(V)(V-E_{\rm Na}) - g_{\rm K} n (V-E_{\rm K})}^{I_{\rm Na,p}+I_{\rm K}\text{-model}} - \overbrace{g_{\rm M} n_{\rm M} (V-E_{\rm K})}^{I_{\rm K(M)}} \\ \dot{n} & = (n_\infty(V) - n)/\tau(V) \\ \dot{n}_{\rm M} & = (n_{\infty,{\rm M}}(V) - n_{\rm M})/\tau_{\rm M}(V) \qquad \text{(slow } {\rm K}^+ \text{ M-current)} \end{array} \tag{7.1}$$

whose excitable and spiking properties are similar to those of the $I_{\rm Na,p}$+$I_{\rm K}$-submodel on a short time scale. However, long-term behavior of the two models may be quite different. For example, the K^+ M-current may result in frequency adaptation during a long train of action potentials. It can change the shape of the I-V relation of the model and result in slow oscillations, post-inhibitory spikes, and other resonator properties even when the $I_{\rm Na,p}$+$I_{\rm K}$-submodel is an integrator. All these interesting phenomena are discussed in this section.

In general, models having fast and slow currents, such as (7.1), can be written in the fast-slow form

$$\begin{array}{rcll} \dot{x} & = & f(x,u) & \text{(fast spiking)} \\ \dot{u} & = & \mu g(x,u) & \text{(slow modulation)} \end{array} \tag{7.2}$$

where vector $x \in \mathbb{R}^m$ describes fast variables responsible for spiking. It includes the membrane potential V, activation and inactivation gating variables for fast currents, etc. Vector $u \in \mathbb{R}^k$ describes relatively slow variables that modulate fast spiking, e.g., gating variable of a slow K^+current, intracellular concentration of Ca^{2+} ions, etc. Small parameter μ represents the ratio of time scales between spiking and its modulation. Such systems often result in bursting activity, and we study them in detail in the next chapter.

7.3.1 Spike-frequency modulation

Slow currents can modulate the instantaneous spiking frequency of a long train of action potentials, as we illustrate in Fig. 7.43a using recordings of a layer 5 pyramidal

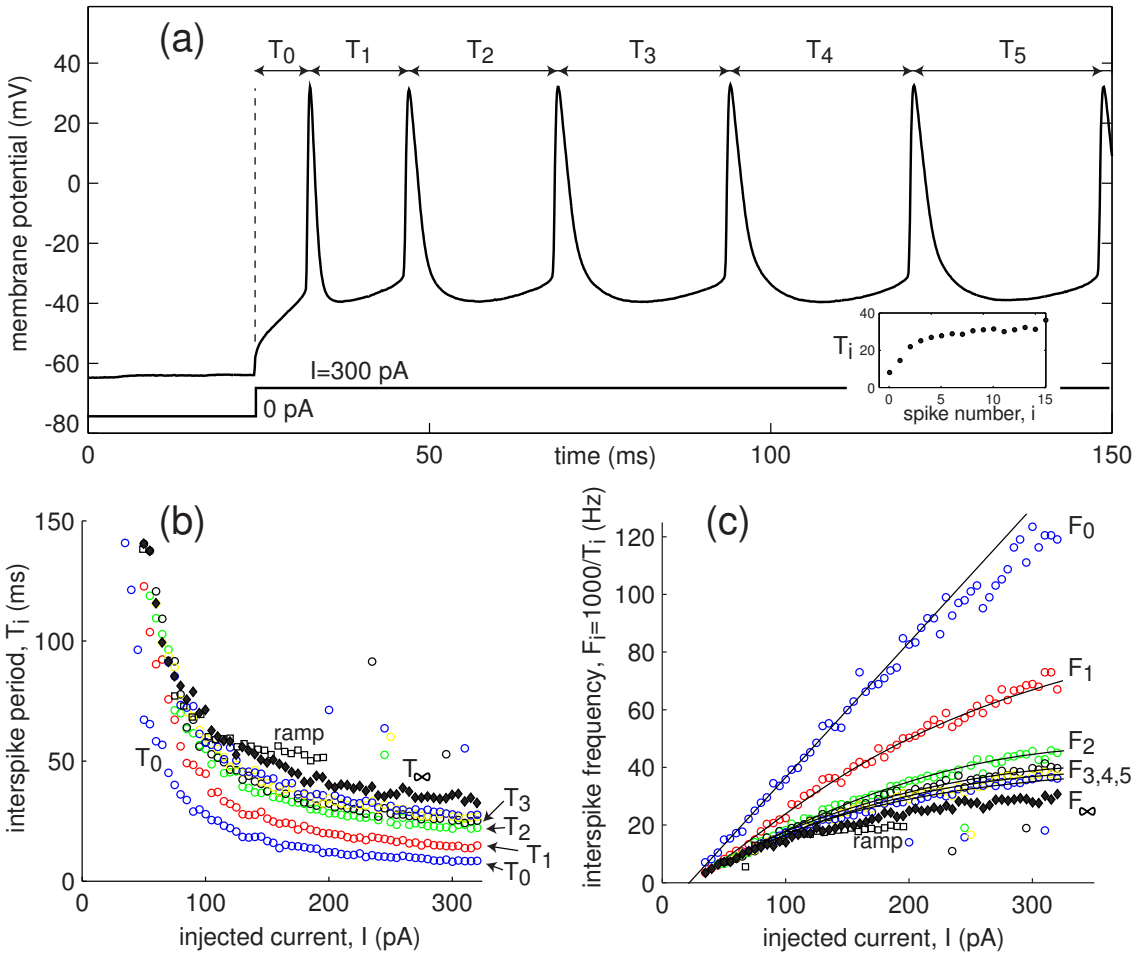

Figure 7.43: Spike-frequency adaptation in layer 5 pyramidal cell (see Fig. 7.3). Ramp data is from Fig. 7.6.

neuron. The neuron generates a train of spikes with increasing interspike interval (see inset in the figure) in response to a long pulse of injected dc-current. In Fig. 7.43b we plot the instantaneous interspike intervals T_i, i.e., the time intervals between spikes number i and $i+1$, as a function of the magnitude of injected current I. Notice that $T_i(I) < T_{i+1}(I)$, meaning that the intervals increase with each spike. The function $T_0(I)$ describes the latency of the first spike, and $T_\infty(I)$ describes the steady-state (asymptotic) interspike period. The instantaneous frequencies are defined as $F_i(I) = 1000/T_i(I)$ (Hz), and they are depicted in Fig. 7.43c. Since the neuron is Class 1 excitable, the F-I curves are square-root parabolas (see Sect. 6.1.2). Notice that $F_0(I)$ is a straight line.

Decrease of the instantaneous spiking frequency, as in Fig. 7.43, is referred to as *spike-frequency adaptation*. This is a prominent feature of cortical pyramidal neurons of the regular spiking (RS) type (Connors and Gutnick 1990), as well as many other types of neurons. In contrast, cortical fast spiking (FS) interneurons (Gibson et al.

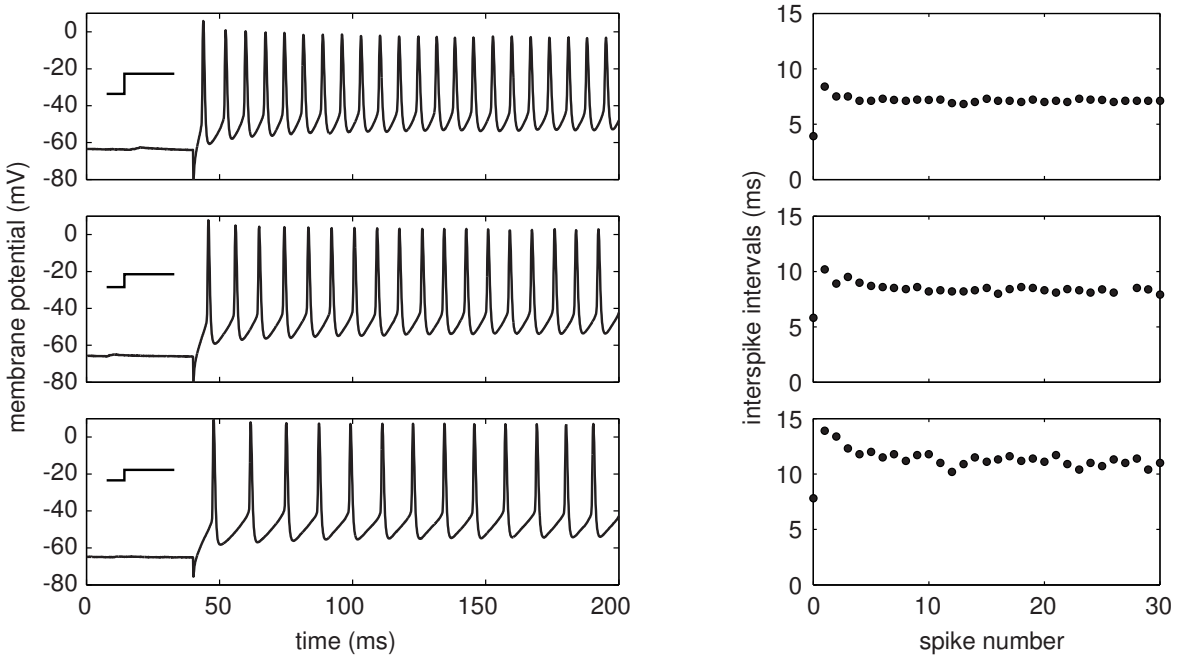

Figure 7.44: Spike-frequency acceleration of a cortical fast spiking (FS) interneuron. Data kindly provided by Barry Connors.

1999) exhibit *spike-frequency acceleration* depicted in Fig. 7.44, i.e., the instantaneous interspike intervals decrease, and the frequency increases with each spike.

Whether a neuron exhibits spike frequency adaptation or acceleration depends on the nature of the slow current (or currents) and how it affects the spiking limit cycle of the fast subsystem. At the first glance, a resonant slow current, e.g., slowly activating K^+ or slowly inactivating Na^+ current, buildups during each spike and provides a negative feedback that should slow down spiking of the fast subsystem. Buildup of a slow amplifying current, e.g., slowly activating Na^+ or inactivating K^+ current, or slow charging of the dendritic tree should have the opposite effect. In the next chapter, devoted to bursting, we will show that this simple rule works for many models, but there are also many exceptions. To understand how the slow subsystem modulates repetitive spiking, we need to consider bifurcations of the fast subsystem in (7.2) treating the slow variable u as a bifurcation parameter.

7.3.2 I-V relation

Slow currents and conductances, though not responsible for the generation of spikes, can mask the true I-V relation of the fast subsystem in (7.2) responsible for spiking. Take, for example, the $I_{\mathrm{Na,p}}$+I_{K}-model with parameters as in Fig. 4.1a (high-threshold K^+ current), so that its I-V curve is non-monotonic with a region of negative slope depicted in Fig. 7.45a. Such a system is near saddle-node on invariant circle bifurcation and it acts as an integrator. Now add a slow K^+ M-current with I-V relation depicted

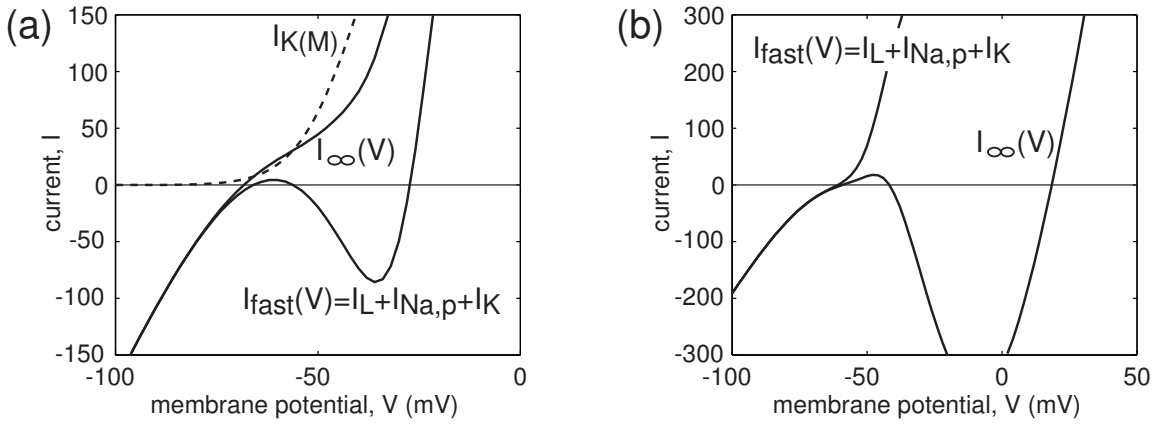

Figure 7.45: Slow conductances can mask the true I-V relation of the spike-generating mechanism. (a) The $I_{\mathrm{Na,p}}$+I_{K}-model with parameters as in Fig. 4.1a has a non-monotonic I-V curve $I_{\mathrm{fast}}(V)$. Addition of the slow K^+ M-current with parameters as in Sect. 2.3.5 and $g_{\mathrm{M}} = 5$ (dashed curve) makes the asymptotic I-V relation, $I_\infty(V)$, of the full $I_{\mathrm{Na,p}}$+I_{K}+$I_{\mathrm{K(M)}}$-model monotonic. (b) Addition of a slow inactivation gate to the K^+ current of the $I_{\mathrm{Na,p}}$+I_{K}-model with parameters as in Fig. 4.1b results in a non-monotonic asymptotic I-V relation of the full $I_{\mathrm{Na,p}}$+I_{A}-model.

as a dash curve in the figure and a time constant $\tau_{\mathrm{M}} = 100$ ms. The spike-generating mechanism of the combined $I_{\mathrm{Na,p}}$+I_{K}+$I_{\mathrm{K(M)}}$-model is described by the fast $I_{\mathrm{Na,p}}$+I_{K}-submodel, so that the neuron continue to have integrator properties, at least on the millisecond time scale. However, the asymptotic I-V relation $I_\infty(V)$ is dominated by the strong $I_{\mathrm{K(M)}}(V)$ and it is monotonic, as if the $I_{\mathrm{Na,p}}$+I_{K}+$I_{\mathrm{K(M)}}$-model is a resonator. The model can indeed exhibit some resonance properties, such as post-inhibitory (rebound) responses, but only on the long time scale of hundreds of milliseconds, i.e., on the time scale of the slow K^+ M-current.

Similarly, we can take a resonator model with a monotonic I-V relation and add a slow amplifying current or a gating variable to get a non-monotonic $I_\infty(V)$, as if the model becomes an integrator. For example, in Fig. 7.45b we use the $I_{\mathrm{Na,p}}$+I_{K}-model with parameters as in Fig. 4.1b (low-threshold K^+ current) and add an inactivation gate to the persistent K^+ current, effectively transforming it into transient A-current. If the inactivation kinetic is sufficiently slow, the $I_{\mathrm{Na,p}}$+I_{A}-model retains resonator properties on the millisecond time scale, i.e., on the time scale of individual spikes. However, its asymptotic I-V relation, depicted in Fig. 7.45b, becomes non-monotonic. Besides spike-frequency acceleration, the model acquires another interesting property – bistability. A single spike does not inactivate I_{A} significantly. A burst of spikes could inactivate the K^+ A-current to such a degree that repetitive spiking becomes sustained.

When a neuronal model consists of conductances operating on drastically different time scales, it has multiple I-V relations, one for each time scale. We illustrate this phenomenon in Fig. 7.46 using the $I_{\mathrm{Na,p}}$+I_{K}+$I_{\mathrm{K(M)}}$-model with activation time constant of 0.01 ms for $I_{\mathrm{Na,p}}$, 1 ms for I_{K}, and 100 ms for $I_{\mathrm{K(M)}}$. The up-stroke of an action

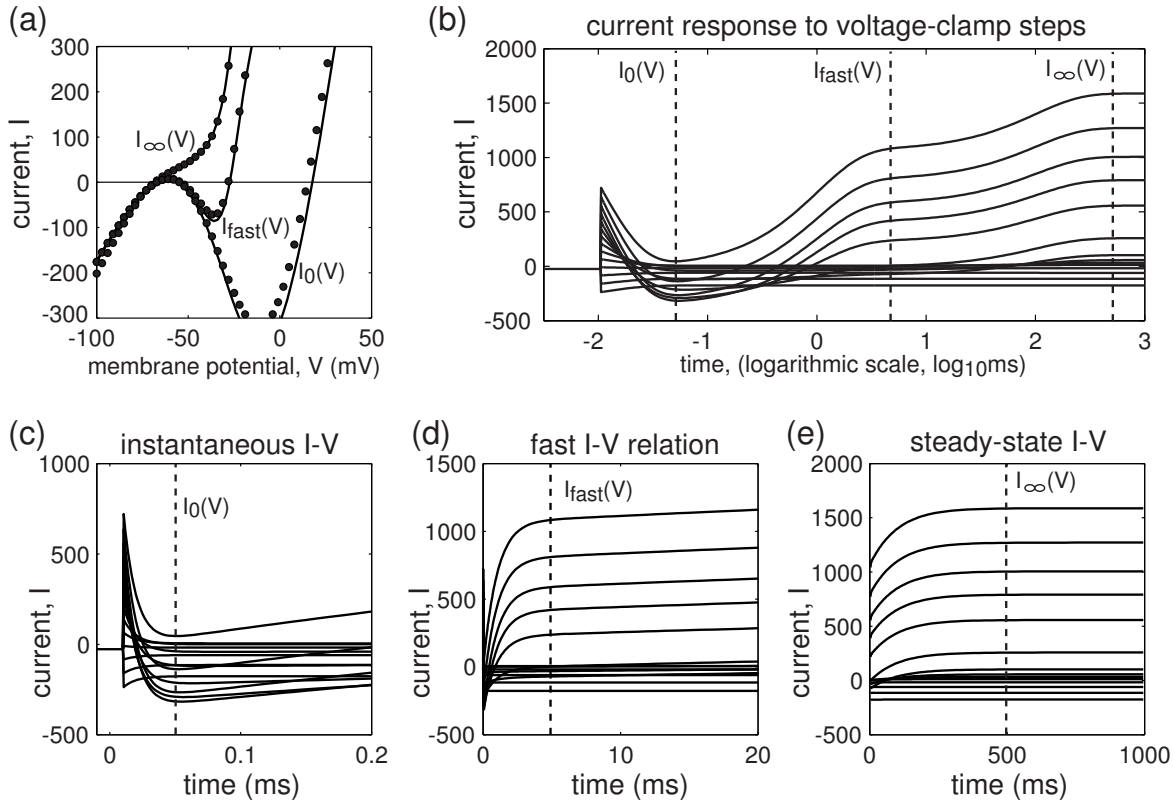

Figure 7.46: (a) The $I_{\rm Na,p}$+$I_{\rm K}$+$I_{\rm K(M)}$-model in Fig. 7.45a has three I-V relations: Instantaneous $I_0(V) = I_{\rm leak}(V) + I_{\rm Na,p}(V)$ describes spike upstroke dynamics. The curve $I_{\rm fast}(V) = I_0(V) + I_{\rm K}(V)$ is the I-V relation of the fast $I_{\rm Na,p}$+$I_{\rm K}$-subsystem responsible for spike-generating mechanism. The curve $I_\infty(V) = I_{\rm fast}(V) + I_{\rm K(M)}(V)$ is the steady-state (asymptotic) I-V relation of the full model. Dots denote values obtained from a simulated voltage-clamp experiment in (b); Notice the logarithmic time scale. Magnifications of current responses are in (c,d,e). Simulated time constants: $\tau_{\rm Na,p}(V) = 0.01$ ms, $\tau_{\rm K}(V) = 1$ ms, $\tau_{\rm M}(V) = 100$ ms.

potential is described only by leak and persistent Na^+ currents, since the K^+ currents do not have enough time to activate during such a short event. During the up-stroke, the model can be reduced to a 1-dimensional system (see Chap. 3) with instantaneous I-V relation $I_0(V) = I_{\rm leak} + I_{\rm Na,p}(V)$ depicted in Fig. 7.46a. Dynamics during and immediately after the action potential is described by the fast $I_{\rm Na,p}$+$I_{\rm K}$-subsystem with its I-V relation $I_{\rm fast}(V) = I_0(V) + I_{\rm K}(V)$. Finally, the asymptotic I-V relation, $I_\infty(V) = I_{\rm fast}(V) + I_{\rm K(M)}(V)$, takes into account all currents in the model.

The three I-V relations determine fast, medium, and asymptotic behavior of a neuron in a voltage-clamp experiment. If the time scales are separated well (they are in Fig. 7.46), all three I-V relations can be measured from a simple voltage-clamp experiment depicted in Fig. 7.46b. We hold the model at $V = -70$ mV and step the command voltage to various values. The values of the current, taken at $t = 0.05$

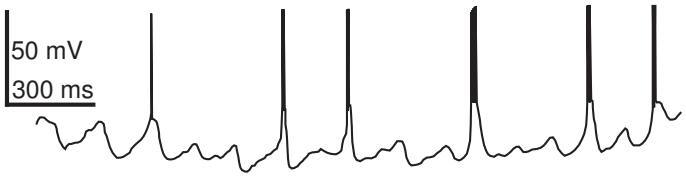

Figure 7.47: Slow subthreshold oscillation of membrane potential of cat thalamocortical neuron evoked by slow hyperpolarization (modified from Roy et al. 1984).

ms, $t = 5$ ms, and $t = 500$ ms in Fig. 7.46b, result in the instantaneous, fast, and steady-state I-V curves, respectively. Notice that the data in Fig. 7.46b is plotted on logarithmic time scale. Various magnifications using linear time scale are depicted in Fig. 7.46c,d, and e. Numerically obtained values of the three I-V relations are depicted as dots in Fig. 7.46a. They approximate the theoretical values quite well because there is a 100-fold separation of time scales in the model.

7.3.3 Slow Subthreshold oscillation

Interactions between fast and slow conductances can result in low-frequency subthreshold oscillation of membrane potential, such as the one in Fig. 7.47, even when the fast subsystem is near a saddle-node bifurcation, acts as an integrator, and cannot have subthreshold oscillations. The oscillation in Fig. 7.47 is caused by the interplay between activation and inactivation of the slow Ca^{2+} T-current and inward h-current, and it is a precursor of bursting activity, which we consider in detail in the next chapter.

We identify three different mechanisms of slow subthreshold oscillations of membrane potential of a neuron.

- The fast subsystem responsible for spiking has a small-amplitude subthreshold limit cycle attractor. The period of the limit cycle may be much larger than the time scale of the slowest variable of the fast subsystem when the cycle is near saddle-node on invariant circle, saddle homoclinic orbit bifurcation, or Bogdanov-Takens bifurcation considered in Chap. 6. In this case, no slow currents or conductances modulating the fast subsystem are needed. However, such a cycle must be near the bifurcation, hence low-frequency subthreshold oscillation exists in a narrow parameter range and it is difficult to be seen experimentally.

- The I-V relation of the fast subsystem has N-shape in the subthreshold voltage range, so that there are two stable equilibria corresponding to two resting states, as e.g., in Fig. 7.36. The slow resonant variable switches the fast subsystem between the states via a hysteresis loop resulting in a subthreshold slow relaxation oscillation.

- If the fast subsystem has a monotonic I-V relation, then stable subthreshold oscillation can result from the interplay between two or more slow variables.

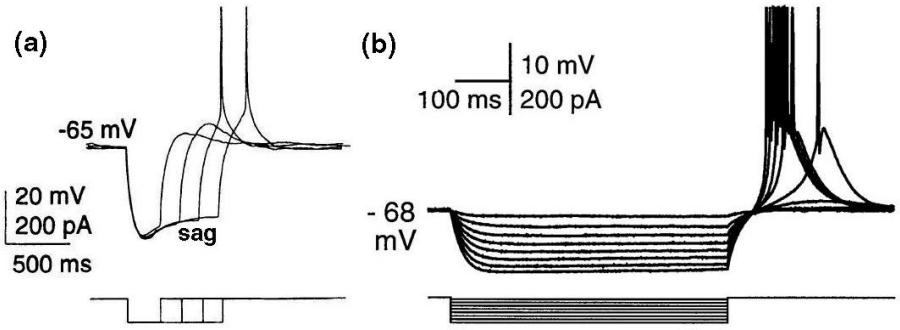

Figure 7.48: Rebound responses to long inhibitory pulses in (a) pyramidal neuron of sensorimotor cortex of juvenile rats (modified from Hutcheon et al. 1996) and (b) rat auditory thalamic neurons (modified from Tennigkeit et al. 1997).

One slow variable is not enough because the entire system can be reduced to a one-dimensional slow equation, as we show in Ex. 7.

7.3.4 Rebound response and voltage sag

A slow resonant current can make a neuron fire a rebound spike or a burst in response to a sufficiently long hyperpolarizing current, even when the spike-generating mechanism of the neuron is near a saddle-node bifurcation and hence has neuro-computational properties of an integrator. For example, the cortical pyramidal neuron in Fig. 7.48a has a slow resonant current $I_{\rm h}$, which opens by hyperpolarization. A short pulse of current does not open enough of $I_{\rm h}$ and results only in a small subthreshold rebound potential. In contrast, a long pulse of current opens enough $I_{\rm h}$, resulting in a strong inward current that produces the voltage sag and, upon termination of stimulation, drives the membrane potential over the threshold.

Similarly, the thalamocortical neuron in Fig. 7.48b has a low-threshold Ca^{2+} T-current $I_{\rm Ca(T)}$ that is partially activated but completely inactivated at rest. A negative pulse of current hyperpolarizes the neuron and deinactivates the T-current, thereby making it available to generate a spike. Notice that there is no voltage sag in Fig. 7.48b because the T-current is deactivated at low membrane potentials. Upon termination of the long pulse of current, the membrane potential returns to the resting state around -68 mV, the Ca^{2+} T-current activates and drives the neuron over the threshold. A distinctive feature of thalamocortical neurons is that they fire a rebound burst of spikes in response to strong negative currents.

Even when the rebound depolarization is not strong enough to elicit a spike, it may increase the excitability of the neuron, so that it fires a spike to an otherwise subthreshold stimulus, as in Fig. 7.49a. This type of post-inhibitory facilitation relies on the slow currents, and not on the resonant properties of the spike-generation mechanism (as in Fig. 7.31). Figure 7.49b demonstrates the inverse property, post-excitatory depression, i.e., a decreased excitability after a transient depolarization. In this seemingly counterintuitive case, a superthreshold stimulation becomes subthreshold when it

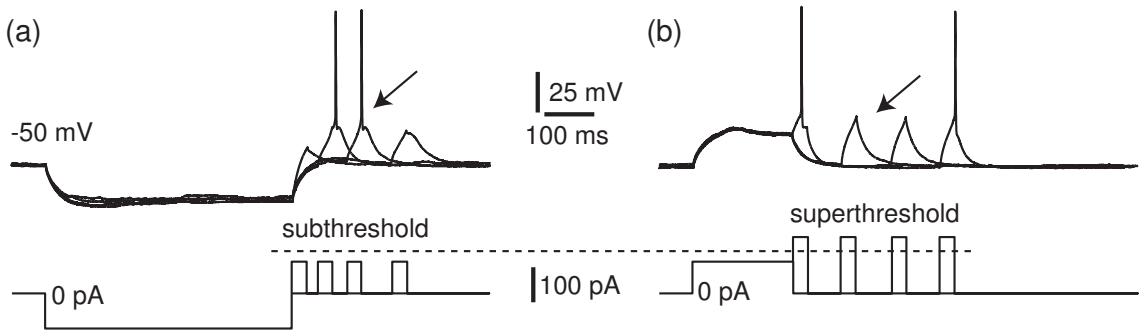

Figure 7.49: Post-inhibitory facilitation (a) and post-excitatory depression (b) in a layer 5 pyramidal neuron (IB type) of rat's visual cortex having slow conductances (*in vitro* recording).

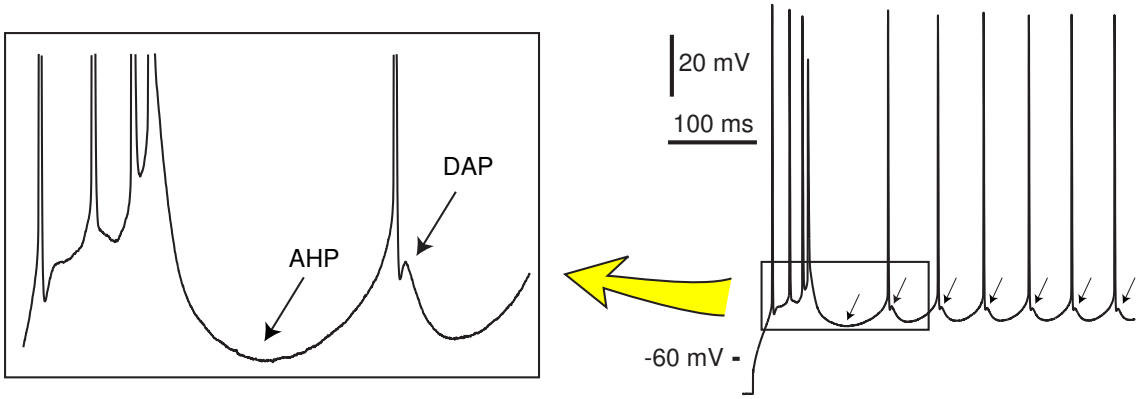

Figure 7.50: Afterhyperpolarizations (AHP) and depolarizing after-potentials (DAPs) in intrinsically bursting (IB) pyramidal neurons of the rat motor cortex.

is preceded by a depolarized pulse, because the pulse partially inactivates Na^+ current and/or activates K^+ current.

7.3.5 AHP and DAP

There could be negative and positive deflections of the membrane potential right after the spike, illustrated in Fig. 7.50 and Fig. 7.51, known as *afterhyperpolarizations* (AHP) and *depolarizing after-potentials* (DAP) or *afterdepolarizations* (ADP). A great effort is usually made to determine the ionic basis of AHPs and DAPs, since it is implicitly assumed that they are generated by slow currents, such as I_{AHP}, or by slow dendritic spikes back-propagating into the soma (which is true for many cortical pyramidal neurons).

Let us consider AHP first. Each spike in the initial burst in Fig. 7.50 presumably activates a slow voltage- or Ca^{2+}dependent outward K^+ current, which eventually stops the burst and hyperpolarizes the membrane potential. During the AHP period, the

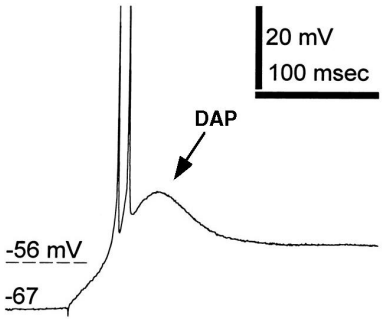

Figure 7.51: Rebound spikes and depolarizing after-potential (DAP) at the break of hyperpolarizing current in thalamocortical neurons of the cat dorsal lateral geniculate nucleus. (data modified from Pirchio et al. 1997, resting potential is -56 mV, holding potential is -67 mV).

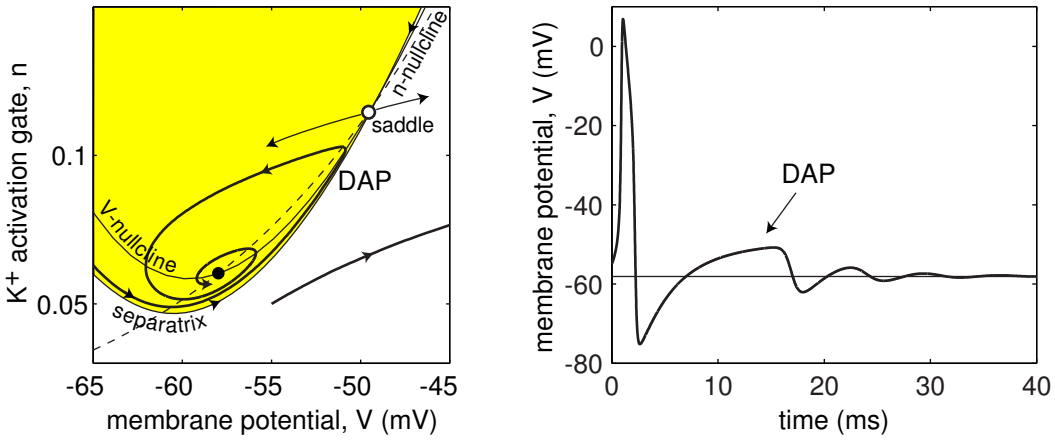

Figure 7.52: A long depolarizing after-potential (DAP) in the $I_{\mathrm{Na,p}}$+I_{K}-model without any slow currents. Parameters as in Fig. 6.53.

slow outward current deactivates and the neuron can fire again. It can switch from bursting to tonic spiking mode due to the incomplete deactivation of the slow current.

Similarly, slow inactivation of the transient Ca^{2+} T-current explains long afterdepolarization in Fig. 7.51: The current was deinactivated by the preceding hyperpolarization, so upon release from the hyperpolarization, it quickly activates and slowly inactivates thereby producing a slow depolarizing wave on which fast spikes can ride. The DAP seen in the figure is the tail of the wave.

There is a tendency in the biological community to misinterpret depolarizing after-potentials as indicators of a slow hidden current that suddenly activates and then slowly deactivates after the spike. Though this may be true in some neurons, slow DAPs can also be generated via nonlinear interplay of fast currents responsible for spiking, rather than via slow currents. One obvious example is the damped oscillation of membrane potential of the $I_{\mathrm{Na,p}}$+I_{K}-model in Fig. 7.52 right after the spike, with the trough and the peak corresponding to an AHP and a DAP. Notice that the duration of the DAP is ten times the duration of the spike even though the model does not have any slow currents. Such a long-lasting effect appears because the trajectory follows the separatrix, comes close to the saddle point, and spends some time there before returning to the stable resting state.

An example in Fig. 7.53 shows the membrane potential of a model neuron slowly

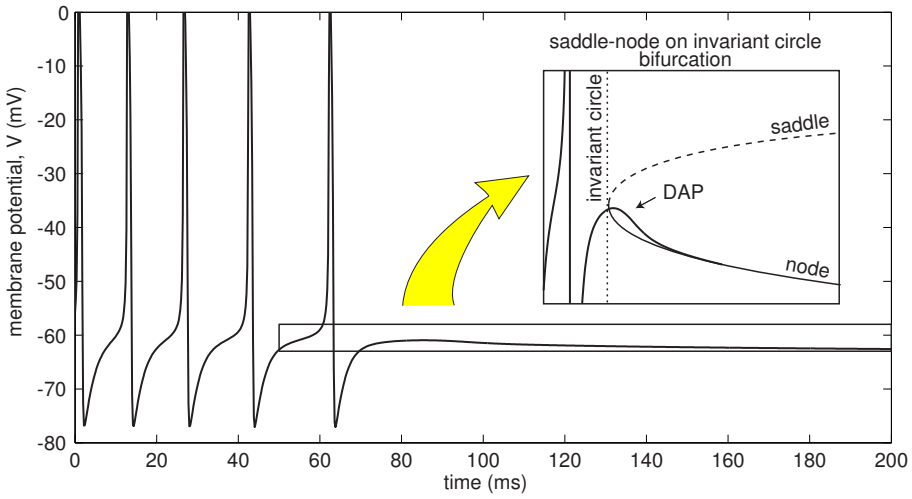

Figure 7.53: Depolarizing after-potential in the $I_{\mathrm{Na,p}}$+I_{K}-model passing slowly through saddle-node on invariant circle bifurcation, as the magnitude of the injected current ramps down.

passing through the saddle-node on invariant circle bifurcation. Because the vector-field is small at the bifurcation, which takes place around $t = 70$ ms, the membrane potential is slowly increasing along the limit cycle and then slowly decreasing along the locus of stable node equilibria, thereby producing a slow DAP. In the next chapter we will show that such DAPs exist in 4 out of 16 basic types of bursting neurons, including thalamocortical relay neurons and R_{15} bursting cells in abdominal ganglion of the mollusk *Aplysia*.